ISSN: 1017-060X (Print)

ISSN: 1735-8515 (Online)

Bulletin of the

Iranian Mathematical Society

Vol. 42 (2016), No. 5, pp. 1127–1142

Title:

The use of inverse quadratic radial basis functions for the solution of an inverse heat problem

Author(s):

F. Parzlivand and A. Shahrezaee

Published by Iranian Mathematical Society
http://bims.ims.ir

Bull. Iranian Math. Soc.
Vol. 42 (2016), No. 5, pp. 1127–1142
Online ISSN: 1735-8515

THE USE OF INVERSE QUADRATIC RADIAL BASIS FUNCTIONS FOR THE SOLUTION OF AN INVERSE HEAT PROBLEM

F. PARZLIVAND AND A. SHAHREZAEE*

(Communicated by Mohammad Asadzadeh)

Abstract. In this paper, a numerical procedure for an inverse problem of simultaneously determining an unknown coefficient in a semilinear parabolic equation subject to the specification of the solution at an internal point along with the usual initial boundary conditions is considered. The method consists of expanding the required approximate solution as the elements of the inverse quadratic radial basis functions (IQ-RBFs). The operational matrix of derivative for IQ-RBFs is introduced and the new computational technique is used for this purpose. The operational matrix of derivative is utilized to reduce the problem to a set of algebraic equations. Some examples are given to demonstrate the validity and applicability of the new method and a comparison is made with the existing results.
Keywords: Collocation, inverse parabolic problem, scattered data, RBFs.
MSC(2010): Primary: 35K05; Secondary: 34K29, 34K28.

1. Introduction

An inverse problem is a general framework that is used to convert observed measurements into information about a physical object or system. For example, if an acoustic plane wave is scattered by an obstacle, and one observes the scattered field far from the obstacle, or in some exterior region, then the inverse problem is to find the shape and material properties of the obstacle. Inverse problems arise in many branches of science and mathematics, including computer vision, natural language processing, machine learning, statistics, statistical inference, geophysics, medical imaging (such as computed axial tomography and EEG/ERP), remote sensing, ocean acoustic tomography, nondestructive testing, astronomy, physics and many other fields [39]. The determination of unknown coefficients in partial

Article electronically published on October 31, 2016.
Received: 23 December 2014, Accepted: 18 July 2015.
*Corresponding author.

differential equations (PDEs) of parabolic type from additional boundary conditions (i.e., measured data taken on the boundary) is well known in literature as inverse coefficient problems (ICPs). Physically, the ICP is the reconstruction of an intraproperty of a medium (for example, conductivity or permittivity) in some bounded regions by using state measurements taken on the boundary. ICPs for semilinear parabolic equations have been studied by many people, for example, by Dehghan [15, 16, 17, 18], Wang and Lin [44], Ramm [38] and Cannon and Lin [5, 6, 9].

1.1. **Problem statement.** In this work, we will consider the following inverse problem of simultaneously finding unknown function $u(x,t)$ and unknown coefficient $p(t)$ from the following parabolic equation:

$$u_t = u_{xx} + qu_x + p(t)u + g(x,t); \qquad 0 < x < 1,\ 0 < t < t_{fin}, \tag{1.1}$$

with the initial and boundary conditions:

$$u(x,0) = u_0(x); \qquad 0 \le x \le 1, \tag{1.2}$$

$$u(0,t) = g_0(t);\ 0 \le t \le t_{fin}, \tag{1.3}$$

$$u(1,t) = g_1(t);\ 0 \le t \le t_{fin}, \tag{1.4}$$

subject to the overspecification at a point in the spatial domain:

$$u(x^\star,t) = E(t); \qquad 0 \le t \le t_{fin}, \tag{1.5}$$

where $t_{fin} > 0$ is constant and $g(x,t)$, $u_0(x)$, $g_0(t)$, $g_1(t)$ and $E(t) \neq 0$ are known functions, q is a known constant and $x^\star$ is a fixed prescribed interior point in $(0,1)$. It is worth pointing that, the problem (1.1)-(1.4) is under-determined and we are forced to impose an additional boundary condition, such that a unique solution pair (u,p) is obtained. Employing the condition (1.5), a recovery of the function $p(t)$ together with the solution $u(x,t)$ can be made possible. The inverse problem (1.1)-(1.5) can be used to describe a heat transfer process with a source parameter $p(t)$, where (1.5) represents the temperature at a given point $x^\star$ in a spatial domain at time t and u is the temperature distribution.

1.2. **A brief review of other methods existing in the literature.** The existence and uniqueness of the solutions to this problem and also some more applications are discussed in [7, 8, 30, 32, 36]. The numerical solution of the problem (1.1)-(1.5) was discussed by several authors. In [16, 17, 18] some well-known finite difference techniques are investigated for solving the problem (1.1)-(1.5). In [43], a method by the reproducing kernel Hilbert space is applied to solve this problem. Authors of [21] used finite difference methods to solve the problem. In [19], several explicit and implicit finite difference procedures have been developed to find the numerical solution of the problem (1.1)-(1.5). Two different numerical procedures are studied in [2]. One of the these procedures obtained by introducing transformation of an unknown function, while the other based on trace functional

Table 1. Some well-known functions that generate RBFs

Name of Radial Basis Function	Definition
Multiquadric(MQ)	$\varphi(r) = \sqrt{c^2 + r^2}$
Inverse Quadratic(IQ)	$\varphi(r) = \frac{1}{(c^2+r^2)}$
Inverse Multiquadric(IMQ)	$\varphi(r) = \frac{1}{\sqrt{c^2+r^2}}$
Gaussian(GA)	$\varphi(r) = \exp(-c^2r^2)$
Thin Plate Splines(TPS)	$\varphi(r) = r^2 \log(r)$

formulation of the problem. In [14], the numerical solution is also considered by use of the third order compact Runge-Kutta method. As for other types of inverse parabolic problems, see e.g. [5, 6, 9, 15, 44, 38].
In this paper, we solve the inverse problem (1.1)-(1.5) by using IQ-RBFs as a truly meshless method. In a meshless (mesh free) method a set of scattered nodes is used instead of meshing the domain of the problem. Although polynomials (e.g., Chebyshev and Legendre) are very powerful tools for interpolating a set of points in one-dimensional domains, the use of these functions is not efficient in higher-dimensional or irregular domains. Also, the use of the RBFs for solving PDEs has some advantages over mesh-dependent methods, such as finite difference methods, finite element methods, finite volume methods and boundary element methods. Since a large portion of the computational time is spent in providing a suitable mesh on the domain of the problem in mesh-dependent methods. The main advantage of numerical methods, which use RBFs over traditional techniques, is the meshless property of these methods. The RBFs method is used actively for solving PDEs. For example see [3, 11, 12, 26, 41, 42]. Also some applications of this approach in solving inverse problems can be found in [1, 29, 34, 35].
The rest of this paper is organized as follows. In Section 2, we describe RBFs and its properties and construct its operational matrix of derivative. In Section 3, the presented technique is used to approximate the solution of the inverse problem (1.1)-(1.5). As a result a set of algebraic equations is formed and the solution of the considered problem is introduced. In Section 4, we give some computational results of numerical experiments with IQ-RBFs method to support our theoretical discussion. The conclusions are discussed in Section 5.

2. Radial basis functions

RBFs were introduced in [23] and they form a primary tool for multivariate interpolation. They are also receiving increased attention for solving PDE in irregular domains. Hardy [24] showed that multiquadrics RBF is related to a consistent solution of the biharmonic potential problem and thus has a physical foundation. Buhmann and Micchelli [4] and Chiu et al. [13] have shown that RBF are related to prewavelets (wavelets that do not have orthogonality properties).

Also, PDEs and ordinary differential equations (ODEs) have been solved using RBFs in recent works [25, 31, 33, 37][39-42].

2.1. **Definition of RBF.** Let $\mathbb{R}^+ = \{x \in \mathbb{R}, x \geq 0\}$, $\|.\|_2$ denotes the Euclidean norm and $\varphi : \mathbb{R}^+ \to \mathbb{R}$ be a continuous function with $\varphi(0) \geq 0$. A RBF on $\mathbb{R}^d$ is a function of the form:

$$\phi_i(\mathbf{x}) = \varphi(\|\mathbf{x} - \mathbf{x}_i\|_2),$$

which depends only on the distance between $\mathbf{x} \in \mathbb{R}^d$ and a fixed point $\mathbf{x}_i \in \mathbb{R}^d$ [2]. So that the RBF ϕ_i is radially symmetric about the center $\mathbf{x}_i$. Let r be the Euclidean distance between a fixed point $\mathbf{x}_i \in \mathbb{R}^d$ and $\mathbf{x} \in \mathbb{R}^d$, i.e. $\|\mathbf{x} - \mathbf{x}_i\|_2$. Some well-known RBFs are listed in Table 1.
The standard RBFs are categorized into two major classes [2, 31].

- Class 1. Infinitely smooth RBFs. These basis functions are infinitely differentiable and involve a parameter, called shape factor (such as multiquadric (MQ), inverse multiquadric (IMQ) and Gaussian (GA)) which needs to be selected so that the required accuracy of the solution is attained.
- Class 2. Infinitely smooth (except at centers) RBFs. These basis functions are not infinitely differentiable. These basis functions are shape parameter free and have comparatively less accuracy than the basis functions discussed in Class 1. Examples are thin plate splines.

Despite research done by many scientists to develop algorithms for selecting the values of c which produce the most accurate interpolation (e.g. see [10, 40]), the optimal choice of shape parameter is still an open question. For example, Franke [22] evaluated about 30 interpolation schemes in two dimensions and found that the most accurate two schemes were MQ and TPS. He suggested the shape parameter $c^2 = 1.25D/\sqrt{N}$ in MQ basis, where D is the diameter of the minimal circle enclosing all data points and N is the number of data points. Hardy [23] recommended $c^2 = 0.815d$ where $d = (1/N)\sum_{i=1}^{N} d_i$ and d_i is the distance between the i-th data point and its nearest neighbor.

2.2. **Function approximation.** Let $X = L^2(\Omega)$ where $\Omega = [0,1] \times [0, t_{fin}]$, the inner product in this space is defined by:

$$\langle f_1(x,t), f_2(x,t)\rangle = \int_0^{t_{fin}} \int_0^1 f_1(x,t)\overline{f_2(x,t)}dxdt,$$

and the norm is as follows:

$$\|f(x,t)\|_2 = \langle f(x,t), f(x,t)\rangle^{\frac{1}{2}} = (\int_0^{t_{fin}} \int_0^1 |f(x,t)|^2 dxdt)^{\frac{1}{2}}.$$

Now, suppose that

$$\{\psi_{11}(x,t), \cdots, \psi_{1M}(x,t), \psi_{21}(x,t), \cdots, \psi_{2M}(x,t), ..., \psi_{N1}(x,t), \cdots, \psi_{NM}(x,t)\} \subset X$$

be the set of IQ- RBFs, where $\psi_{ij}(x,t)=\frac{1}{(x-x_i)^2+(t-t_j)^2+c^2}$ and

$$Y=span\{\psi_{11}(x,t),\cdots,\psi_{1M}(x,t),\psi_{21}(x,t),\cdots,\psi_{2M}(x,t),...,\psi_{N1}(x,t),\cdots,\psi_{NM}(x,t)\},$$

and $f(x,t)$ be an arbitrary element in X. Since Y is a finite dimensional vector space, f has the unique best approximation out of Y such as $f_{NM}\in Y$, that is [28]:

$$\forall y\in Y,\ \|f-f_{NM}\|_2\leq\|f-y\|_2.$$

Since $f_{NM}\in Y$, there exist unique coefficients $c_{11},...,c_{1M},c_{21},...,c_{2M}...,$ $c_{N1},...,c_{NM}$ such that:

$$f(x,t)\simeq f_{NM}(x,t)=\sum_{i=1}^{N}\sum_{j=1}^{M}c_{ij}\psi_{ij}(x,t)=C^T\Psi_{NM}(x,t)=\Psi_{NM}^T(x,t)C,$$

where C and $\Psi_{NM}(x,t)$ are vectors with the form:

$$C=[c_{11},...,c_{1M},c_{21},...,c_{2M}...,c_{N1},...,c_{NM}]^T, \tag{2.1}$$

$$\Psi_{NM}(x,t)=[\psi_{11}(x,t),\cdots,\psi_{1M}(x,t),\psi_{21}(x,t),\cdots,\psi_{NM}(x,t)]^T, \tag{2.2}$$

where T indicates transposition.

2.3. **The operational matrix of derivative.** The differentiation with respect to x of vectors $\Psi_{NM}(x,t)$ in (2.2) can be expressed as:

$$\frac{\partial}{\partial x}\Psi_{NM}(x,t)=D_N(x)\Psi_{NM}^{(2)}(x,t), \tag{2.3}$$

where $\Psi_{NM}^{(k)}(x,t)=[\psi_{11}^k(x,t),\psi_{12}^k(x,t),\cdots,\psi_{NM}^k(x,t)]^T; k=2,3$ and $D_N(x)$ is $N\times M$ operational matrix of derivative with respect to x for IQ-RBFs. The matrix $D_N(x)$ can be obtained as:

$$\frac{\partial}{\partial x}\Psi_{NM}(x,t)=[\frac{\partial}{\partial x}\psi_{11}(x,t),\cdots,\frac{\partial}{\partial x}\psi_{NM}(x,t)]^T=\begin{bmatrix}-2(x-x_1)\psi_{11}^2(x,t)\\ \vdots\\ -2(x-x_1)\psi_{1M}^2(x,t)\\ -2(x-x_2)\psi_{21}^2(x,t)\\ \vdots\\ -2(x-x_2)\psi_{2M}^2(x,t)\\ \vdots\\ -2(x-x_N)\psi_{N1}^2(x,t)\\ \vdots\\ -2(x-x_N)\psi_{NM}^2(x,t)\end{bmatrix}. \tag{2.4}$$

Comparing (2.3) and (2.4), we can write:

$$\frac{\partial}{\partial x}\Psi_{NM}(x,t)=\begin{bmatrix} M_1(x) & 0 & \cdots & 0 \\ 0 & M_2(x) & \cdots & 0 \\ \vdots & \vdots & \ddots & \vdots \\ 0 & 0 & \cdots & M_N(x) \end{bmatrix}\begin{bmatrix} \psi_{11}^2(x,t) \\ \vdots \\ \psi_{1M}^2(x,t) \\ \psi_{21}^2(x,t) \\ \vdots \\ \psi_{2M}^2(x,t) \\ \vdots \\ \psi_{N1}^2(x,t) \\ \vdots \\ \psi_{NM}^2(x,t) \end{bmatrix},$$

where $M_i(x)=-2(x-x_i)I_M; i=1,2,...,N$ and I_M is $M\times M$ identity matrix. Therefore we have:

$$D_N(x)=\begin{bmatrix} M_1(x) & 0 & \cdots & 0 \\ 0 & M_2(x) & \cdots & 0 \\ \vdots & \vdots & \ddots & \vdots \\ 0 & 0 & \cdots & M_N(x) \end{bmatrix}. \tag{2.5}$$

Similarly, the differentiation with respect to t of vectors $\Psi_{NM}(x,t)$ in (2.2) can be expressed as:

$$\frac{\partial}{\partial t}\Psi_{NM}(x,t)=D_M(t)\Psi_{NM}^{(2)}(x,t), \tag{2.6}$$

where $D_M(t)=diag(N_1(t),N_2(t),\cdots,N_M(t))$ and $N_i(t)=-2(t-t_i)I_{N\times N}; i=1,2,...,M$.
And

$$\frac{\partial^2}{\partial x^2}\Psi_{NM}(x,t)=\begin{bmatrix} 8(x-x_1)^2\psi_{11}^3(x,t)-2\psi_{11}^2(x,t) \\ \vdots \\ 8(x-x_1)^2\psi_{1M}^3(x,t)-2\psi_{1M}^2(x,t) \\ 8(x-x_2)^2\psi_{21}^3(x,t)-2\psi_{21}^2(x,t) \\ \vdots \\ 8(x-x_2)^2\psi_{2M}^3(x,t)-2\psi_{2M}^2(x,t) \\ \vdots \\ 8(x-x_N)^2\psi_{N1}^3(x,t)-2\psi_{N1}^2(x,t) \\ \vdots \\ 8(x-x_N)^2\psi_{NM}^3(x,t)-2\psi_{NM}^2(x,t) \end{bmatrix}. \tag{2.7}$$

So we have:

$$\frac{\partial^2}{\partial x^2}\Psi_{NM}(x,t) = 2D_N^2(x)\Psi_{NM}^{(3)}(x,t) - 2\Psi_{NM}^{(2)}(x,t), \tag{2.8}$$

Similarly:

$$\frac{\partial^2}{\partial t^2}\Psi_{NM}(x,t) = 2D_M^2(t)\Psi_{NM}^{(3)}(x,t) - 2\Psi_{NM}^{(2)}(x,t). \tag{2.9}$$

3. Description of the new computational technique

To use the IQ-RBFs for solving the inverse problem (1.1)-(1.5), at first we use the following transformation.

3.1. The employed transformation.

Consider the following transformations [43]:

$$w(x,t) = u(x,t)\exp(\frac{q}{2}x)r(t), \tag{3.1}$$

$$r(t) = \exp(-\int_0^t (p(s) - \frac{q^2}{4})ds), \tag{3.2}$$

we reduce the original inverse problem (1.1)-(1.5) to the following auxiliary problem:

$$w_t = w_{xx} + r(t)\exp(\frac{q}{2}x)g(x,t); \qquad 0 < x < 1,\ 0 < t < t_{fin}, \tag{3.3}$$

$$w(x,0) = u_0(x)\exp(\frac{q}{2}x); \qquad 0 < x < 1, \tag{3.4}$$

$$w(0,t) = g_0(t)r(t); \qquad 0 < t < t_{fin}, \tag{3.5}$$

$$w(1,t) = g_1(t)\exp(\frac{q}{2}x)r(t); \qquad 0 < t < t_{fin}, \tag{3.6}$$

subject to:

$$r(t) = \frac{w(x^\star,t)}{E(t)}\exp(-\frac{q}{2}x^\star); \qquad 0 < x < 1,\ 0 < t < t_{fin}. \tag{3.7}$$

It is easy to show that the original inverse problem (1.1)-(1.5) is equivalent to the auxiliary problem (3.3)-(3.7). Obviously, Eq. (3.3) has only one unknown function $w(x,t)$ and a suitable form to apply the IQ-RBFs method.

3.2. **The computational framework.** Let $x_1 = 0$, $x_N = 1$ and $\Omega_1 = \{x_i | \, 0 < x_i < 1, \; i = 2, 3, \cdots, N-1\}$ be a set of scattered nodes on $[0,1]$ and $t_1 = 0$ and $\Omega_2 = \{t_j | \, 0 < t_j \leq t_{fin}, \; j = 2, 3, \cdots, M\}$ be a set of scattered nodes on $[0, t_{fin}]$. Then the solution of the problem (3.3)-(3.7) by using IQ-RBFs is considered as follows:

$$w(x,t) \simeq \sum_{i=1}^{N} \sum_{j=1}^{M} w_{ij} \psi_{ij}(x,t) = W^T \Psi_{NM}(x,t), \tag{3.8}$$

where $\Psi_{NM}(x,t)$ is the vector of IQ-RBFs defined in (2.2) and
$W = [w_{11}, w_{12}, ..., w_{NM}]^T$ is an unknown vector which remains to be determined. Using (2.6), (2.8) and (3.8) in (3.3), we obtain:

$$\begin{aligned} W^T D_M(t) \Psi^{(2)}_{NM}(x,t) &= 2W^T D^2_N(x) \Psi^{(3)}_{NM}(x,t) - 2W^T \Psi^{(2)}_{NM}(x,t) \\ &+ \frac{\exp(\frac{q}{2}(x - x^\star)) g(x,t)}{E(t)} W^T \Psi_{NM}(x^\star, t). \end{aligned} \tag{3.9}$$

And using (3.8) in (3.4)-(3.6) yields:

$$W^T \Psi_{NM}(x, 0) = u_0(x) \exp(\frac{q}{2} x), \tag{3.10}$$

$$W^T \Psi_{NM}(0, t) = \frac{\exp(-\frac{q}{2} x^\star) g_0(t)}{E(t)} W^T \Psi_{NM}(x^\star, t), \tag{3.11}$$

$$W^T \Psi_{NM}(1, t) = \frac{\exp(\frac{q}{2}(x - x^\star)) g_1(t)}{E(t)} W^T \Psi_{NM}(x^\star, t). \tag{3.12}$$

The collocation technique is used for finding the unknown vector W.
We collocate (3.9) in $(N-2) \times (M-1)$ points $\{(x_i, t_j) | x_i \in \Omega_1, \; t_j \in \Omega_2\}$, to get:

$$\begin{aligned} W^T D_M(t_j) \Psi^{(2)}_{NM}(x_i, t_j) &= 2W^T D^2_N(x_i) \Psi^{(3)}_{NM}(x_i, t_j) - 2W^T \Psi^{(2)}_{NM}(x_i, t_j) \\ &+ \frac{\exp(\frac{q}{2}(x_i - x^\star)) g(x_i, t_j)}{E(t_j)} W^T \Psi_{NM}(x^\star, t_j); \; x_i \in \Omega_1, t_j \in \Omega_2. \end{aligned} \tag{3.13}$$

Now, collocation (3.10)-(3.12) in N points x_i, $i = 1, ..., N$ and $M-1$ points t_j, $j = 2, ..., M$, yields:

$$W^T \Psi_{NM}(x_i, 0) = u_0(x_i) \exp(\frac{q}{2} x_i); \; i = 1, 2, ..., N, \tag{3.14}$$

$$W^T \Psi_{NM}(0, t_j) = \frac{\exp(-\frac{q}{2} x^\star) g_0(t_j)}{E(t_j)} W^T \Psi_{NM}(x^\star, t_j); \; j = 2, 3, ..., M, \tag{3.15}$$

$$W^T \Psi_{NM}(1, t_j) = \frac{\exp(\frac{q}{2}(1 - x^\star)) g_1(t_j)}{E(t_j)} W^T \Psi_{NM}(x^\star, t_j); \; j = 2, 3, ..., M, \tag{3.16}$$

Equations (3.13)-(3.16) give a $N \times M$ system of nonlinear algebraic equations which can be solved for the $N \times M$ unknown coefficients w_{ij}, using the Newtons iterative method. It is well known that the initial guesses for Newtons iterative method are very important. For our problem, by using $w(x,0) = u_0(x)\exp(\frac{q}{2}x)$ and Equation (3.8), we choose the initial guesses such that $W^T\Psi_{NM}(x_i,0) = u_0(x_i)\exp(\frac{q}{2}x_i)$; $i = 1, 2, ..., N$. Solving this system, the unknown function of $w(x,t)$ can be found. Having $w(x,t)$ determined, then the value of $u(x,t)$ can be computed by using the equation (3.1) where $r(t)$ is given in (3.7). And finally the approximate value of $p(t)$ is:

$$p(t) = \frac{q^2}{4} - \frac{r'(t)}{r(t)}.$$

4. Test examples

In this section, the theoretical considerations introduced in the previous sections will be illustrated with some examples. For all of the three examples, the true solutions are available. Example 1 was first considered in [32] by using the several finite difference schemes and was also solved in [1] by using Crank-Nicolson method and in [34] by using a high order compact finite difference scheme. we compare our findings with the numerical results obtained in [1, 32, 34]. Examples 2 and 3 were considered in [14, 31, 33]. We compare our findings with the numerical results in [31], which have been shown to be comparable or superior to those of [14, 33].
In the process of computation, all the symbolic and numerical computations are performed by using Maple 13. We tested the accuracy and stability of the method presented in this paper by performing the mentioned method for different values of N and M. To study the convergence behavior of the RBFs method, we apply the following laws:
(1) The error **Error** is described using:
$\mathbf{Error}(u) = \sqrt{\frac{\sum_{i=1}^{N}\sum_{j=1}^{M}(u(x_i,t_j)-\tilde{u}(x_i,t_j))^2}{\sum_{i=1}^{N}\sum_{j=1}^{M}(u(x_i,t_j))^2}}$
(2) The root mean square (RMS) is described using:
$RMS(u) = \sqrt{\frac{1}{NM}\sum_{i=1}^{N}\sum_{j=1}^{M}|u(x_i,t_j) - \tilde{u}(x_k,t_j)|^2}$,
where u is the exact value and $\tilde{u}$ is the RBFs approximation.

4.1. Example 1.

We solve the problem (1.1)-(1.5) with [14, 15, 19]:
$T = 1$, $x^\star = 0.25$, $q = 0$, $g(x,t) = (\pi^2 - (t+1)^2)\exp(-t^2)(\cos(\pi x) + \sin(\pi x))$, $u_0(x) = \cos(\pi x)+\sin(\pi x)$, $g_0(t) = \exp(-t^2)$, $g_1(t) = -\exp(-t^2)$, $E(t) = \sqrt{2}\exp(-t^2)$ for which the exact solution is $u(x,t) = \exp(-t^2)(\cos(\pi x) + \sin(\pi x))$ and $p(t) = 1 + t^2$.
In Tables 2 and 3, the results for $u(x,t)$ in $t = 1.0$ and p are shown for $\triangle x = 0.02$ and $\triangle t = 10^{-4}$, using the formulas [19] and [15]. Also the corresponding results obtained using the IQ-RBFs method with equidistance collocation points with $x_i = (i-1)/(N-1)$ and $t_j = (j-1)/(M-1)$, $N = M = 16$ and $c = 50$ are

TABLE 2. Absolute values of error for u from Example 1.

x	(1,3) FTCS [19]	(1,5) FTCS [19]	(3,1) BTCS [19]	Grandall [19]	Crank-Nicolson [15]	Present Method
0.15	2.1×10^{-3}	2.7×10^{-6}	3.8×10^{-3}	3.2×10^{-6}	6.3×10^{-6}	1.1×10^{-10}
0.35	2.5×10^{-3}	3.0×10^{-6}	3.5×10^{-3}	2.9×10^{-6}	6.6×10^{-6}	8.0×10^{-10}
0.55	2.3×10^{-3}	3.4×10^{-6}	3.9×10^{-3}	2.8×10^{-6}	6.8×10^{-6}	5.8×10^{-10}
0.75	2.1×10^{-3}	3.2×10^{-6}	4.1×10^{-3}	3.3×10^{-6}	7.4×10^{-6}	5.3×10^{-10}
0.95	2.6×10^{-3}	3.7×10^{-6}	4.0×10^{-3}	3.6×10^{-6}	7.1×10^{-6}	5.3×10^{-10}

TABLE 3. Absolute values of error for p from Example 1.

t	(1,3) FTCS [19]	(1,5) FTCS [19]	(3,1) BTCS [19]	Grandall [19]	Crank-Nicolson [15]	Present Method
0.1	4.4×10^{-3}	5.0×10^{-5}	6.1×10^{-3}	5.6×10^{-5}	6.8×10^{-5}	1.1×10^{-8}
0.2	4.2×10^{-3}	4.9×10^{-5}	5.3×10^{-3}	5.4×10^{-5}	6.7×10^{-5}	6.9×10^{-10}
0.3	4.1×10^{-3}	4.7×10^{-5}	6.0×10^{-3}	5.4×10^{-5}	6.8×10^{-5}	7.3×10^{-10}
0.4	3.8×10^{-3}	4.5×10^{-5}	5.7×10^{-3}	5.1×10^{-5}	6.5×10^{-5}	1.4×10^{-9}
0.5	3.8×10^{-3}	4.5×10^{-5}	5.5×10^{-3}	4.8×10^{-5}	6.2×10^{-5}	2.2×10^{-10}

TABLE 4. The comparison between the exact, methods in [14] and IQ-RBFs solution for $u(x, 0.5)$ for Example 1.

x	Implicit error [14]	Explicit error [14]	Runge-Kutta error [14]	Present Method	Exact u
0.2	1.494974×10^{-3}	3.604912×10^{-4}	9.667994×10^{-4}	1.1×10^{-10}	1.087831
0.4	3.608708×10^{-3}	8.443811×10^{-4}	2.113957×10^{-4}	5.4×10^{-9}	9.813462×10^{-1}
0.6	6.434342×10^{-3}	1.479397×10^{-3}	3.713589×10^{-4}	6.5×10^{-9}	5.002090×10^{-1}
0.8	7.701922×10^{-3}	1.796665×10^{-3}	4.568415×10^{-4}	2.2×10^{-10}	1.722955×10^{-1}

TABLE 5. **Error** and RMS errors for u and p for Example 1 with $c = 50$.

Error	$N = 6, M = 7$	$N = 8, M = 10$	$N = 10, M = 9$	$N = 11, M = 11$	$N = 16, M = 16$
$RMS(u)$	6.239E–04	2.066E–05	3.531E–07	2.222E–07	3.243E–10
Error(u)	8.105E–04	2.879E–05	4.582E–07	2.881E–07	4.201E–10
$RMS(p)$	5.029E–02	1.178E–03	1.863E–04	2.104E–05	3.385E–08
Error(p)	3.580E–02	8.470E–04	1.335E–04	1.514E–05	2.450E-08

presented in these tables. Table 4 shows the comparison between the exact solution, IQ-RBFs solution with equidistance collocation points, $N = M = 16$ and $c = 50$ and approximate solution result from methods in [14] in $t = 0.5$. Table 5 shows the **Error** and RMS error values for various values of N and M. It can be obtained from Table 5 and Fig. 1 that the accuracy increases with the increase of the number of collocation points.

4.2. **Example 2.** We solve the problem (1.1)-(1.5) with [21, 43]:
$T = 1$, $x^\star = 0.5$, $q = 2$, $g(x,t) = ((\frac{\pi^2}{4} - t)\sin(\frac{\pi}{2}x) - \pi\cos(\frac{\pi}{2}x))\exp(t)$, $u_0(x) = \sin(\frac{\pi}{2}x)$, $g_0(t) = 0$, $g_1(t) = \exp(t)$, $E(t) = \frac{\sqrt{2}}{2}\exp(t)$ for which the exact solution is $u(x,t) = \sin(\frac{\pi}{2}x)\exp(t)$ and $p(t) = 1 + t$.
For our method, the finite difference method (FDM) [21] and the method in [43], (RMS) errors of the $u(x,t)$ and $p(t)$, and CPU time are presented in Table 6. From this table, it is easy to obtain good results when the number of collocation points are large, also when the CPU time is short. In addition, the graphs of the

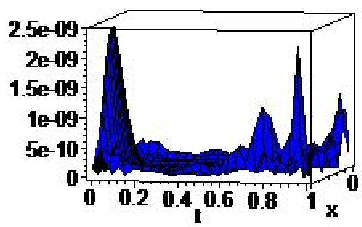

(a) Graph of $|u(x,t) - \tilde{u}(x,t)|$ for $N = M = 16$.

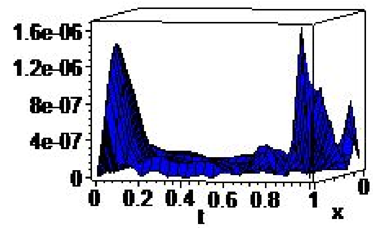

(b) Graph of $|u(x,t) - \tilde{u}(x,t)|$ for $N = M = 11$.

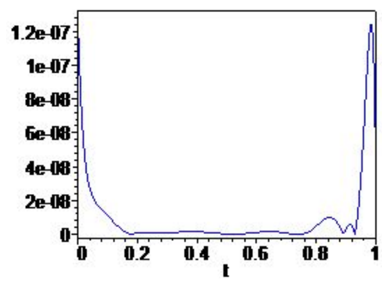

(c) Graph of $|p(t) - \tilde{p}(t)|$ for $N = M = 16$.

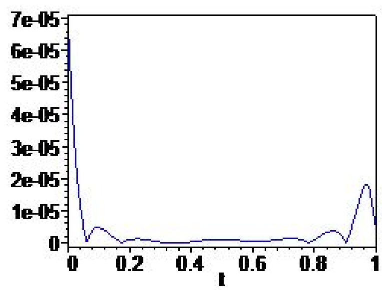

(d) Graph of $|p(t) - \tilde{p}(t)|$ for $N = M = 11$.

FIGURE 1. Graph of absolute error for u and p by using IQ-RBF for Example 1 with $c = 50$.

absolute error functions $|u(x,t) - \tilde{u}(x,t)|$ and $|p(t) - \tilde{p}(t)|$ are plotted in Fig. 2 with $N = M = 8$.

4.3. **Example 3.** Consider the problem (1.1)-(1.5) with the following conditions [2, 43]:
$T = 1$, $x^\star = 0.5$, $q = 2$, $g(x,t) = -(2 + xt^2)\exp(t)$, $u_0(x) = x$, $g_0(t) = 0$, $g_1(t) = \exp(t)$, $E(t) = \frac{1}{2}\exp(t)$ for which the exact solution is $u(x,t) = x\exp(t)$ and $p(t) = 1 + t^2$.
For our method, the finite difference method (FDM) [2] and the method in [43], (RMS) errors of the $u(x,t)$ and $p(t)$, and CPU time are presented in Table 6. From this table, it is easy to obtain good results when the number of collocation points are large, also when the CPU time is short. In addition, the graphs of the absolute error functions $|u(x,t) - \tilde{u}(x,t)|$ and $|p(t) - \tilde{p}(t)|$ are plotted in Fig. 2 with $N = M = 8$.

TABLE 6. CPU time, RMS(u) and RMS(p) for Example 2 with equidistance collocation points and $c = 50$.

Method	$N \times M$	RMS(u)	RMS(p)	CPU times (s)
Method [21]	26×26	1.9×10^{-3}	6.8×10^{-2}	0.577
	30×30	1.6×10^{-3}	5.8×10^{-2}	1.029
	40×40	1.2×10^{-3}	4.3×10^{-2}	2.433
	50×50	9.5×10^{-4}	3.4×10^{-2}	5.367
	56×56	8.4×10^{-4}	3.0×10^{-2}	8.237
	66×66	7.1×10^{-4}	2.5×10^{-3}	15.495
Method [43]	3×3	3.7×10^{-4}	5.9×10^{-4}	0.249
	4×4	1.1×10^{-4}	1.1×10^{-4}	0.795
	5×5	3.7×10^{-5}	9.6×10^{-5}	1.966
	6×6	1.6×10^{-5}	6.3×10^{-5}	4.009
	7×7	8.0×10^{-6}	5.2×10^{-5}	7.504
	8×8	4.4×10^{-6}	4.7×10^{-5}	12.777
Our method	7×7	2.8×10^{-6}	2.7×10^{-5}	6.600
	8×8	1.6×10^{-7}	6.8×10^{-6}	7.500
	10×14	4.0×10^{-9}	2.4×10^{-7}	19.832
	16×15	5.2×10^{-13}	1.2×10^{-11}	61.052

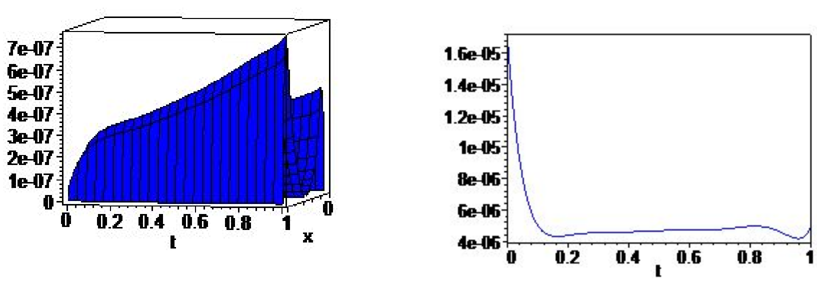

(a) Graph of $|u(x,t) - \tilde{u}(x,t)|$. (b) Graph of $|p(t) - \tilde{p}(t)|$.

FIGURE 2. Graph of absolute error for u and p by using IQ-RBF for Example 2 with $c = 50$ and for $N = M = 8$.

5. Conclusion

In this paper we presented a numerical scheme for solving a parabolic PDE with a time-dependent coefficient subject to an extra measurement. The IQ-RBFs on interval $[0, 1]$ and $[0, T]$ were employed. The new algorithm proposed in the

TABLE 7. CPU time, RMS(u) and RMS(p) for Example 3 with equidistance collocation points and $c = 50$.

Method	$N \times M$	RMS(u)	RMS(p)	CPU times (s)
Method [2]	20×20	$1.4{\times}10^{-3}$	$1.9{\times}10^{-1}$	0.219
	26×26	$1.0{\times}10^{-3}$	$1.4{\times}10^{-1}$	0.578
	34×34	$7.5{\times}10^{-4}$	$1.0{\times}10^{-1}$	1.388
	42×42	$5.9{\times}10^{-4}$	$8.2{\times}10^{-2}$	2.871
	50×50	$4.9{\times}10^{-4}$	$6.7{\times}10^{-2}$	5.274
	56×56	$4.3{\times}10^{-4}$	$6.0{\times}10^{-2}$	8.035
Method [43]	3×3	$8.6{\times}10^{-4}$	$6.2{\times}10^{-3}$	0.141
	4×4	$3.3{\times}10^{-4}$	$2.2{\times}10^{-3}$	0.437
	5×5	$1.3{\times}10^{-4}$	$7.2{\times}10^{-4}$	1.138
	6×6	$6.0{\times}10^{-5}$	$2.5{\times}10^{-4}$	2.277
	7×7	$3.2{\times}10^{-5}$	$1.2{\times}10^{-4}$	4.212
	8×8	$2.0{\times}10^{-5}$	$9.1{\times}10^{-5}$	7.207
Our method	7×7	$1.4{\times}10^{-6}$	$1.5{\times}10^{-5}$	2.900
	8×8	$3.2{\times}10^{-7}$	$4.3{\times}10^{-6}$	4.724
	9×12	$9.8{\times}10^{-8}$	$1.1{\times}10^{-6}$	9.005
	13×12	$3.6{\times}10^{-8}$	$2.1{\times}10^{-7}$	20.701

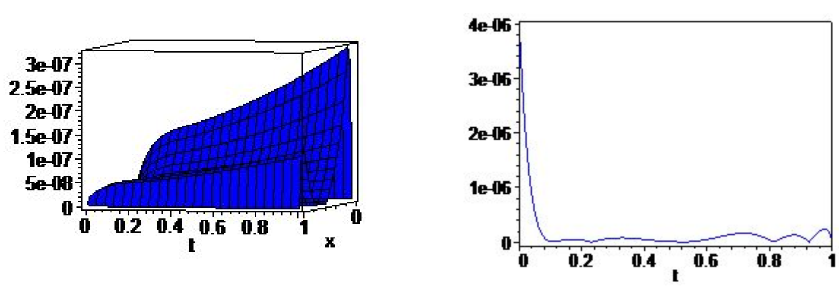

(a) Graph of $|u(x,t) - \tilde{u}(x,t)|$. (b) Graph of $|p(t) - \tilde{p}(t)|$.

FIGURE 3. Graph of absolute error for u and p by using IQ-RBF for Example 3 with $c = 50$ and for $N = M = 8$.

current paper was tested on several examples from the literature. Comparing with other methods, the results of numerical examples demonstrate that this method is more accurate than some existing methods.

Acknowledgements

We would like to thank the anonymous referees for their valuable comments and helpful suggestions to improve the final manuscript.

References

[1] H. Azari and F. Parzlivand, Determination of the coefficient in the advection diffusion equation using collocation and radial basis function, *Univ. J. Integral Equations* **2** (2014) 20–29.

[2] E. C. Baran, Numerical procedures for determining of an unknown parameter in parabolic equation, *Appl. Math. Comput.* **162** (2005), no. 3, 1219–1226.

[3] D. Brown, L. Ling, E. Kansa and J. Levesley, On approximate cardinal preconditioning methods for solving PDEs with radial basis functions, *Eng. Anal. Bound. Elem.* **29** (2005) 343–353.

[4] M. D. Buhmann and C. A. Micchelli, Multiquadric interpolation improved. Advances in the theory and applications of radial basis functions, *Comput. Math. Appl.* **24** (1992), no. 12, 21–25.

[5] J. R. Cannon and Y. Lin, Determination of parameter $p(t)$ in Hölder classes for some semilinear parabolic equations, *Inverse Problems* **4** (1988), no. 3, 595–606.

[6] J. R. Cannon and Y. Lin, An inverse problem of finding a parameter in a semi-linear heat equation, *J. Math. Anal. Appl.* **145** (1990), no. 2, 470–484.

[7] J. R. Cannon, Y. Lin and S. Xu, Numerical procedures for the determination of an unknown coefficient in semi-linear parabolic differential equations, *Inverse Problems* **10** (1994), no. 2, 227–243.

[8] J. R. Cannon, Y. Lin and S. Wang, Determination of source parameter in parabolic equations, *Meccanica* **27** (1992) 85–94.

[9] J. R. Cannon and H. M. Yin, Numerical solutions of some parabolic inverse problems, *Numer. Methods Partial Differential Equations* **2** (1990), no. 2, 177–191.

[10] R. E. Carlson and T. A. Foley, Interpolation of track data with radial basis methods, *Comput. Math. Appl.* **24** (1992), no. 12, 27–34.

[11] S. Chantrasirivan, Cartesian grid method using radial basis functions for solving Poisson, Helmholtz, and diffusion convection equations, *Eng. Anal. Bound. Elem.* **28** (2004) 1417–1425.

[12] W. Chen and M. Tanaka, A meshless, integration-free and boundary only RBF technique, *Comput. Math. Appl.* **4** (2002), no. 3-5, 379–391.

[13] C. K. Chiu, J. Stoeckler and J. D. Ward, Analytic wavelets generated by radial functions, *Adv. Comput. Math.* **5** (1996), no. 1, 95–123.

[14] F. Davoodi, A. Abbas Nejad, A. Shahrezaee and M. J. Maghrebi, Control parameter estimation in a semi-linear parabolic inverse problem using a high accurate method, *Appl. Math. Comput.* **218** (2011), no. 5, 1798–1804.

[15] M. Dehghan, Numerical solution of one-dimensional parabolic inverse problem, *Appl. Math. Comput.* **136** (2003), no. 2-3, 333–344.

[16] M. Dehghan, Determination of a control parameter in the two-dimensional diffusion equation, *Appl. Numer. Math.* **37** (2001), no. 4, 489–502.

[17] M. Dehghan, An inverse problem of finding a source parameter in a semilinear parabolic equation, *Appl. Math. Model.* **25** (2001) 743–754.

[18] M. Dehghan, Determination of a control function in three-dimensional parabolic equations, *Math. Comput. Simulation* **61** (2003), no. 2, 89–100.

[19] M. Dehghan, Finding a control parameter in one-dimensional parabolic equation, *Appl. Math. Comput.* **135** (2003), no. 2-3, 491–503.

[20] M. Dehghan and A. Shokri, A meshless method for numerical solution of the one-dimensional wave equation with an integral condition using radial basis functions, *Numer. Algorithms* **52** (2009), no. 3, 461–477.
[21] A. Fatullayev and E. Can, Numerical procedures for determining unknown source parameter in parabolic equations, *Math. Comput. Simulation* **54** (2000), no. 1-3, 159–167.
[22] R. Franke, A Critical Comparison of Some Methods for Interpolation of Scattered Data, PhD thesis, Naval Postgraduate School Monterey, California, 1979.
[23] R. L. Hardy, Multiquadratic equation of topography and other irregular surfaces, *J. Geophys. Res.* **76** (1971) 1905–1915.
[24] R. L. Hardy, Theory and applications of the multiquadric biharmonic method: 20 years of discovery, *Comput. Math. Appl.* **19** (1990), no. 8-9, 163–208.
[25] S. U. Islam, S. Haqb and A. Ali, A meshfree method for the numerical solution of the RLW equation, *J. Comput. Appl. Math.* **223** (2009), no. 2, 997–1012.
[26] E. Kansa and Y. C. Hon, Circumventing the ill-conditioning problem with multiquadric radial basis functions: applications to elliptic partial differential equations, *Comput. Math. Appl.* **39** (2000), no. 7-8, 123–137.
[27] A. J. Khattak, S. I. A. Tirmizi and S. U. Islam, Application of meshfree collocation method to a class of nonlinear partial differential equations, *Eng. Anal. Bound. Elem.* **33** (2009), no. 5, 661–667.
[28] E. Kreyszig, Introductory Functional Analysis with Applications, John Wiley & Sons Press, New York, 1978.
[29] J. Li, Application of radial basis meshless methods to direct and inverse biharmonic boundary value problems, *Commun. Numer. Methods Eng.* **21** (2005), no. 4, 169–182.
[30] S. Liu and R. Triggiani, Global uniqueness and stability in determining the damping and potential coefficients of an inverse hyperbolic problem, *Nonlinear Anal. Real World Appl.* **12** (2011), no. 3, 1562–1590.
[31] N. Mai-Duy and T. Tran-Cong, Numerical solution of differential equations using multiquadric radial basis function networks, *Neural Netw.* **14** (2001) 185–199.
[32] J. A. MacBain and J. B. Bednar, Existence and uniqueness properties for the one-dimensional magnetotellurics inversion problem, *J. Math. Phys.* **27** (1986), no. 2, 645–649.
[33] K. Parand, S. Abbasbandy, S. Kazem and J. A. Rad, A novel application of radial basis functions for solving a model of first-order integro-ordinary differential equation, *Commun. Nonlinear Sci. Numer. Simul.* **16** (2011), no. 11, 4250–4258.
[34] F. Parzlivand and A. M. Shahrezaee, Numerical solution of an inverse reaction diffusion problem via collocation method based on radial basis functions, *Appl. Math. Model.* **39** (2015), no. 13, 3733–3744.
[35] F. Parzlivand, A. M. Shahrezaee, Gaussian radial basis functions for the solution of an inverse problem of mixed parabolic-hyperbolic type, *Eur. J. Pure Appl. Math.* **8** (2015), no. 2, 239–254.
[36] A. I. Prilepko and V. V. Soloev, Solvability of the inverse boundary value problem of finding a coefficient of a lower order term in a parabolic equation, *J. Differential Equ.* **23** (1987) 136–143.
[37] H. Power, M. Zerroukat and C. Chen, A numerical method for heat transfer problems using collocation and radial basis functions, *Internat. J. Numer. Methods Engrg.* **42** (1998) 1263–1278.
[38] A. G. Ramm, An inverse problem for the heat equation, *Proc. Roy. Soc. Edinburgh Sect.* **123** (1993), no. 6, 973–976.
[39] A. G. Ramm, Mathematical and Analytical Techniques with Application to Engineering, Springer, NewYork, 2005.
[40] S. Rippa, An algorithm for selecting a good value for the parameter c in radial basis function interpolation, *Adv. Comput. Math.* **11** (1999), no. 2-3, 193–210.

[41] S. A. Sarra, Adaptive radial basis function method for time dependent partial differential equations, *Appl. Numer. Math.* **54** (2005), no. 1, 79–94.

[42] C. Shu, H. Ding, and K. S. Yeo, Solution of partial differential equations by a global radial basis function-based differential quadrature method, *Eng. Anal. Bound. Elem.* **28** (2004) 1217–1226.

[43] W. Wang, B. Han and M. Yamamoto, Inverse heat problem of determining time-dependent source parameter in reproducing kernel space, *Nonlinear Anal. Real World Appl.* **14** (2013), no. 1, 875–887.

[44] S. Wang and Y. Lin, A finite-difference solution to an inverse problem for determining a control function in a parabolic partial differential equation, *Inverse Problems* **5** (1989), no. 4, 631–640.

(Farzaneh. Parzlivand) Department of Mathematics, Alzahra University, Vanak, Post Code 19834, Tehran, Iran.

E-mail address: fparzlivand@gmail.com

(Alimardan Shahrezaee) Department of Mathematics, Alzahra University, Vanak, Post Code 19834, Tehran, Iran.

E-mail address: ashahrezaee@alzahra.ac.ir